J Fail. Anal. and Preven. (2011) 11:158–166
DOI 10.1007/s11668-010-9422-z

TECHNICAL ARTICLE—PEER-REVIEWED

Fatigue Failure Analysis of a Grease-Lubricated Roller Bearing from an Electric Motor

Zhi-Qiang Yu · Zhen-Guo Yang

Submitted: 16 August 2010 / in revised form: 30 November 2010 / Published online: 22 December 2010

Abstract The grease-lubricated roller bearing of an electric motor that drove a supply blower suddenly failed during operation. In order to identify the causes of the failure, a variety of characterizations were carried out. The failed surfaces of the bearing were observed visually and microscopically, and the characteristics of the lubricating grease were also investigated. Results showed that the surface of the inner ring of the bearing contained contact fatigue damage, and was covered with a multitude of debris and contact fatigue pits. What's more, the lubricating grease was subjected to severe thermally induced degradation due to high service temperature, which consequently resulted in the decrease of the lubricating capacity of the grease. Thus, the lubricant film in the roller/raceway contacts was not formed effectively and the lubrication of the roller bearing was poor. As a result, serious local wear as well as contact fatigue damage were brought about on the roller and raceway and the wear finally led to the failure of the bearing.

Keywords Bearing failure · Contact fatigue damage · Greases lubrication · Lubricant degradation

Introduction

Roller bearings are significant components of supply blower motors and play a critical role in normal operation of the blower, although many factors can lead to failures of a roller bearing [1–4], failures of lubricating grease may be the predominant cause of failure. The failed greases generally suffered from physical, chemical, and thermal degradations during bearing operation [5–8], and the degradation brought about the loss of lubricating capacities, especially under high temperatures and high velocity conditions. Physical changes are commonly involved with the increase of oil separation, the loss of thickener structure, and the reduction of base oil content [9]. Chemical changes are mainly due to oxidation of base oil and thickener and loss of antioxidant additives, which will consequently increase the amount of acidic species and high-viscosity products. Komatsuzaki et al. [10] showed that the loss of base oil was generally caused by the evaporation of volatile oxidation products and was the predominant factor controlling the lubrication life of grease in cylindrical roller bearings.

The most common failure event that results from failed lubricating greases in rolling-element bearings is surface contact fatigue [11]. According to this failure mode, cracks usually initiate at or near the contact surfaces, and subsequently form microscopic pits, which will then act as the stress concentration sites for further damages [3, 11] during continuing bearing operation. What's more, such stress concentration sites on the contact surfaces interact with other pre-existing defects including handling damage, surface inclusions, and dents to formed solid particles entrapped in the lubrication fluid [3]. These particles will accelerate the initiation of cracks and promote additional debris production [12].

This article will present a failure analysis of one grease-lubricated bearing that was sealed at the driving end of a supply blower motor that had a rotation speed of 990 r/min in the electric power unit. The bearing was a cylindrical roller bearing with 18 rolling elements. The face material

Z.-Q. Yu (✉) · Z.-G. Yang
Department of Materials Science, Fudan University, Shanghai, China
e-mail: yuzhiqiang@fudan.edu.cn

of the bearing was GCr15 bearing steel, while the cage material was an alloy of copper and zinc. The lubricating grease was lithium based containing MoS_2 particles. During its operation, the bearing suddenly failed when its operation temperature exceeded the warning limit of 70 °C. After that, the lubricating grease which was found on the side of the raceway of the detached failed bearing was agglomerated, semisolid, and heavily. Meanwhile, the raceway surface of the inner ring of the bearing showed the signs of contact fatigue and wear. Thus, in order to identify the causes of the failure, the lubricating grease used in the failed bearing was collected and then inspected by Fourier transform infrared spectroscopy (FT-IR), X-ray diffraction (XRD), and thermogravimetric analysis (TGA), while the micromorphologies and chemical compositions of the wear faces were examined by scanning electron microscopy (SEM) and energy dispersive spectroscopy (EDS). Based on the analysis and relevant discussion, failure prevention methodologies for similar grease-lubricated roller bearing were developed.

Investigation Methods

FT-IR with KBr discs, XRD with Co K_α radiation, and TGA under N_2 purge were applied to investigate the structural and thermal characteristics of the greases. Besides that, microstructures of the greases and the wear marks on the bearing inner-ring surface were observed by SEM. Chemical compositions of the bearing material were determined by photoelectric direct reading spectrometry and the material hardness (HRC) was also measured.

Observation Results and Analysis

Figure 1 displays the external morphology of the detached bearing. It is obvious that the raceway surfaces of the bearing inner ring were worn heavily and there were large number of pits and debris on the surface. The inner-ring surfaces were a red-brown color and appeared polished which may the result of direct contact between the rollers and the raceway during operation. Also, the lubricating grease was found to be solidified and pushed out of the bearing track.

Characterizations of the Lubricating Grease

Samples of used greases from the failed bearing were identified by FT-IR, XRD, SEM with EDS, and TGA, and was then compared with the fresh greases.

Fig. 1 Dismounted samples of failure bearing

FT-IR Analysis

Figure 2 shows the FT-IR spectra of used and fresh grease samples. The fresh grease spectrum (Fig. 2a) shows characteristic absorbance peaks of carboxylate stretch at 1597 cm^{-1} and hydroxyl at 3441 cm^{-1} due to the presence of hydroxystearate thickener. The bands at 1460 and 1377 cm^{-1} were assigned to CH vibrations from the base oil [9]. On contrast, the intense carbonyl (C=O) band at 1709 cm^{-1} occurred in the infrared spectrum of the used grease (Fig. 2b), which was from the oxidation of base oil and thickener in the greases. In addition, that the thickener peaks were reduced to a broad ill-defined band indicates that the sample of used grease was mainly composed of base oil and carbonyl-containing degradation products. Hence, it can be concluded that the grease in the roller/raceway contact suffered heavily thermo-oxidation degradation under the high temperature.

The thermo-oxidation degradation of the grease followed the free radicals reaction mechanism [13], seen in Eq. 1. The alkyl free radicals ($R^\bullet$) were formed in the grease in the initial phase of the oxidation reaction with the temperature increase during the bearing rolling. In general, the reaction speed was very slow.

$$RH \xrightarrow{\Delta} R^\bullet + H^\bullet \qquad \text{(Eq 1)}$$

where RH denotes the base oil and thickener in grease, $R^\bullet$ and $H^\bullet$ were free radicals of the alkyl and hydrogen, respectively.

The reaction between the alkyl free radicals and oxygen gas occurred quickly to generate peroxide groups ($ROO^\bullet$) after alkyl radicals formation during the chain propagation. Successively, the reaction occurred between the peroxide groups and RH (the base oil and thickener) by direct abstracting hydrogen atoms from RH and then generated

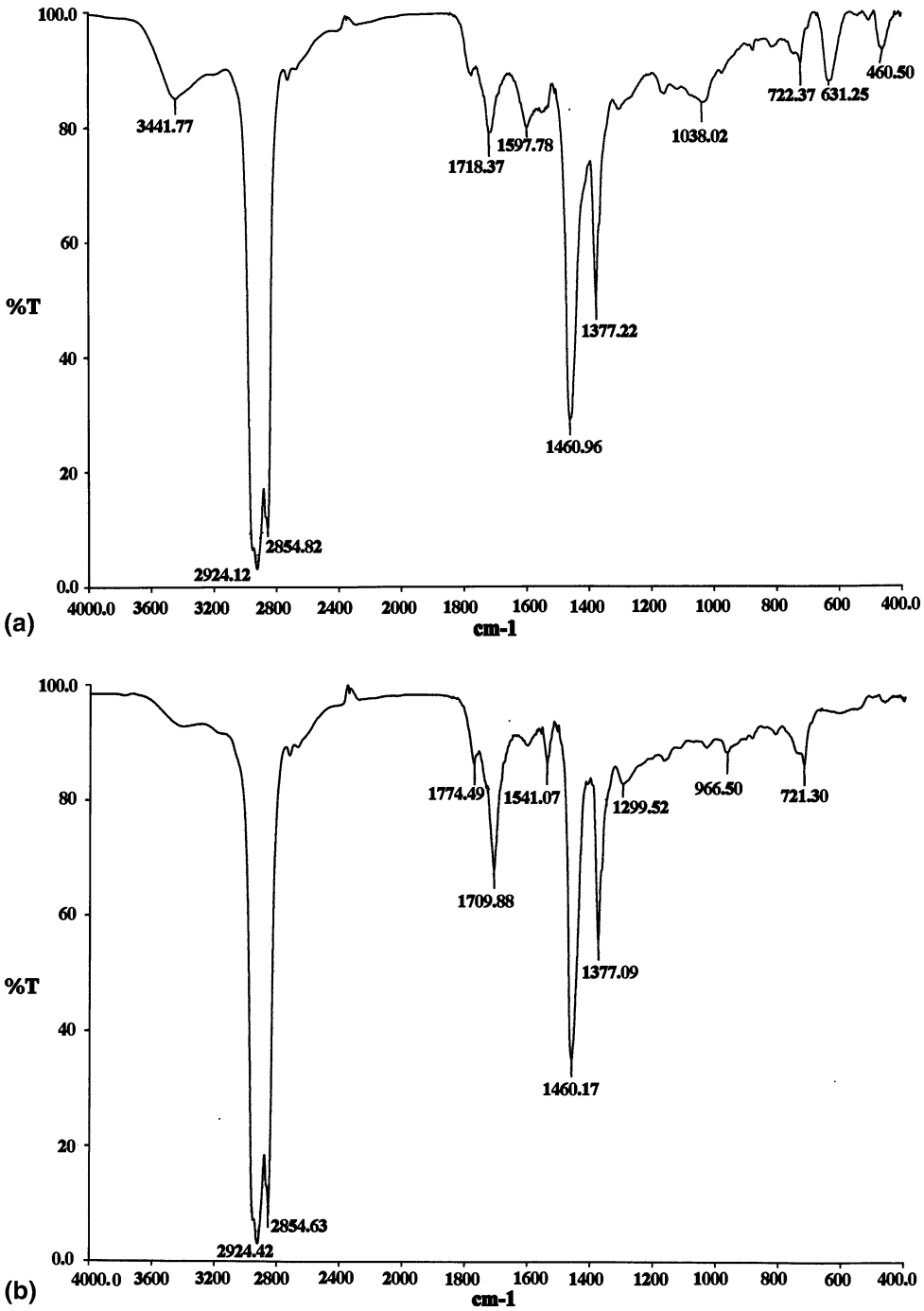

Fig. 2 FT-IR spectra of (**a**) fresh and (**b**) used grease sample

the hydrogen peroxide and secondary alkyl free radicals, as shown in reactions (2) and (3). In this way, the reactions would not cease until the termination of the chain occurred via reaction with the hydrogen free radical, and/or mutual coupling, as shown in reactions (4) and (5), respectively.

$$R^{\bullet} + O_2 \rightarrow ROO^{\bullet} \quad \text{(Eq 2)}$$

$$ROO^{\bullet} + RH \rightarrow ROOH + R^{\bullet} \quad \text{(Eq 3)}$$

$$R^{\bullet} + H^{\bullet} \rightarrow RH \quad \text{(Eq 4)}$$

$$R^{\bullet} + R^{\bullet} \rightarrow R - R \quad \text{(Eq 5)}$$

When the temperature increased the hydrogen peroxide (ROOH) decomposed into alkyl-oxygen radicals ($RO^{\bullet}$) and hydroxyl radicals ($HO^{\bullet}$), as shown in reaction (6), below. These groups could further react with RH to produce the final alkyl radicals ($R^{\bullet}$), as shown in

reactions (7) and (8), which would return to the above chain propagation again. As a result, thermal-oxidative stability of the lubricating grease was repeatedly decreased.

$$\mathrm{ROOH} \xrightarrow{\Delta} \mathrm{RO}^{\bullet} + \mathrm{HO}^{\bullet} \quad \text{(Eq 6)}$$

$$\mathrm{HO}^{\bullet} + \mathrm{RH} \rightarrow \mathrm{H_2O} + \mathrm{RO}^{\bullet} \quad \text{(Eq 7)}$$

$$\mathrm{RO}^{\bullet} + \mathrm{RH} \rightarrow \mathrm{ROH} + \mathrm{R}^{\bullet} \quad \text{(Eq 8)}$$

Thus, during the chain termination the content of the carbonyl-containing oxidation products including acidic species and high-viscosity products increased in the lubricating grease and heavily deteriorated the lubricating properties of the grease.

According to Xue et al. [14], the intensity of C=O peaks was directly proportional to the degradation degree of the grease. As illustrated in Fig. 2b, the C=O peak was sharp and the peak intensity was high (compared with the fresh grease, see Fig. 2a). Consequently, it could be concluded that large amounts of compounds containing C=O group were produced in the used greases, i.e., the greases in the roller/raceway contacts were oxidized and degraded heavily.

XRD Analysis and SEM Observation

Figure 3a and b shows the XRD patterns of the fresh and used grease sample, respectively. From the X-ray analysis, it is clear that there were significant differences between the patterns. The strongest diffraction peak from the fresh sample, as shown in Fig. 3a, appeared at about $2\theta = 14°$, corresponding planar spacing $d = 0.63$ nm, another strong diffraction peak presents at about $2\theta = 26°$, corresponding planar spacing $d = 0.34$ nm. According to PDF cards, they could be attributed to (100) and (101) crystalline planes of the molybdenum disulfide (MoS_2). In addition, some weak diffraction peaks of MoS_2 also appeared in this XRD profile. This means that the fresh grease was a lithium lubricating grease containing MoS_2. Actually, SEM observation and EDS analysis of the fresh grease confirmed this fact as well. Figure 4a and b shows SEM and EDS results of the fresh grease sample, respectively. As shown in Fig. 4a, there were some even particulates (arrows) with a size of around 5 μm dispersing in a fine microstructure of the greases. The EDS results indicated that those particulates consisted of molybdenum (Mo) and sulfur (S) elements, namely MoS_2. In comparison, the intensity of

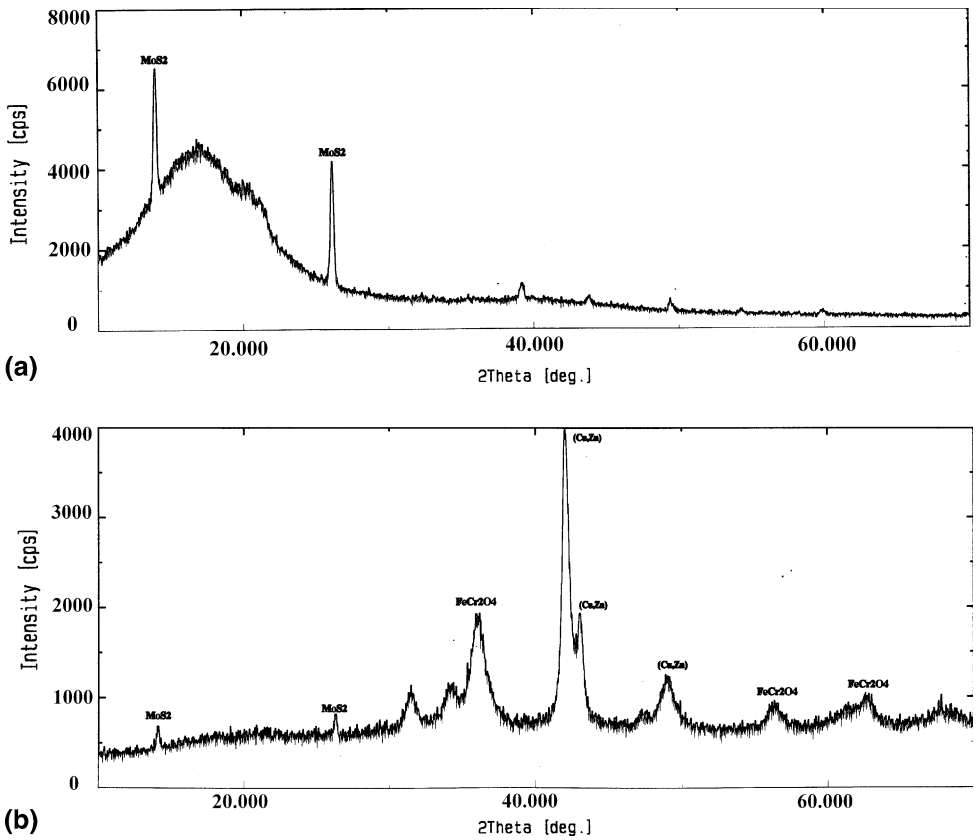

Fig. 3 X-ray analysis of (**a**) fresh and (**b**) used grease sample

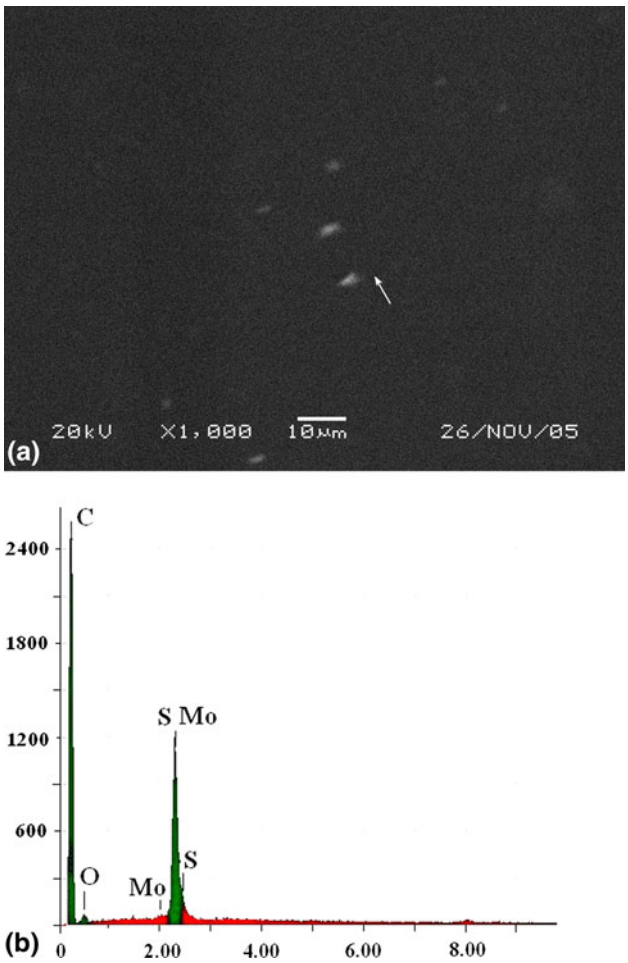

Fig. 4 SEM and EDS of the fresh grease sample. (**a**) SEM micrograph and (**b**) EDS analysis

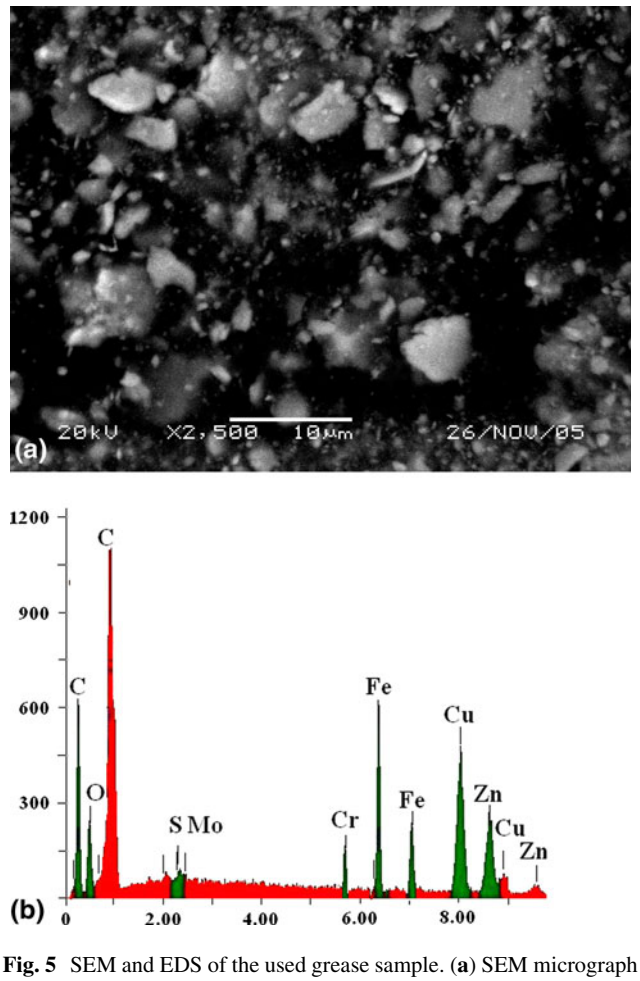

Fig. 5 SEM and EDS of the used grease sample. (**a**) SEM micrograph and (**b**) EDS analysis

MoS_2 diffraction peaks was decreased significantly in XRD patterns of the used grease sample, as shown in Fig. 3b. In it, the strongest diffraction peak (2θ = 42°, d = 0.21 nm) could be attributed to (110) crystalline plane of the Cu–Zn intermetallic (identified by PDF cards). At the same time, the weak diffraction peaks of $FeCr_2O_4$ (about 2θ = 36°, d = 0.25 nm, 2θ = 56°, d = 0.16 nm, etc.) also existed in Fig. 3b. It revealed that the used grease sample was a complex mixture of compounds like MoS_2, Cu–Zn intermetallic, $FeCr_2O_4$, and so on. Figure 5a shows SEM micrograph of the used greases. Compared to the micrograph of the fresh grease (Fig. 4a), it is obvious that there were a large amount of irregular particulates in the used greases. The EDS analysis of different particulates showed that these particulates mainly contained elements like Cu, Zn, Fe, Mo, S, etc. (see Fig. 5b). It can be inferred that the uneven particulates were resulted from agglomeration of different compounds made from these elements, which was consistent with above XRD results of the used grease. The presence of metallic particulates, particularly those containing copper, would further accelerate the oxidation of the base oil and thickener, and consequently degraded the grease [9]. Actually, the metallic elements Cu, Zn, Fe, etc. in the used grease were mainly derived from the bearing (ring or roller) and the cage materials (Cu, Zn alloy). That is to say, the roller bearings had suffered a serious extent of wear. With regard to MoS_2 diffraction peaks being weakened in XRD curve of the used grease sample, it suggested that the contents of MoS_2 particulates in the used grease had decreased since the content of metal debris increased in the grease. Thus, the relative value of the MoS_2 content was reduced. In addition, another factor may be that part of the MoS_2 particulates had been dissociated from the grease and agglomerated on the raceways due to loss of the grease network structure induced by thermal degradation/oxidation.

The above analysis demonstrated that the phase components of the used grease samples were quite different with that of fresh ones. The structure of the grease in bearing had significantly changed during the bearing operation.

Thermogravimetric Analysis

The thermal stability of the fresh and used grease sample under ambient conditions was analyzed by TGA in order to further verify the above results. The TGA of the grease were carried out under N_2 with a heating rate of 20 °C/min from 50 to 900 °C. Figure 6a and b show the weight loss curves of the fresh and used grease samples, respectively. The fresh grease showed a simple degradation step starting at around 210 °C and ending at 783 °C with a weight loss by 98.55%, i.e., the grease was basically completely decomposed. While for the used greases, as shown in Fig. 6b, the thermal decomposition started at temperature of 116.6 °C with a decrease by 93.4 °C compared with that of the fresh grease, which is attributed to low-molecular compounds resulted from the thermal degradation of the used grease during the bearing operation. This showed that the thermal stability of the used greases was lower than that of the fresh one. In addition, there was still a residue of 60.6% (wt.%) at final degradation temperature around 887 °C though the temperature was shifted up to 104 °C higher as compared to fresh greases. Then, the residue constituent was examined by ICP-AES. The results indicated that its compositions were copper (around 36 wt.%), zinc (27.6 wt.%), iron (10.2 wt.%), and their oxides. This further confirmed the above XRD and EDS analysis results of the used greases.

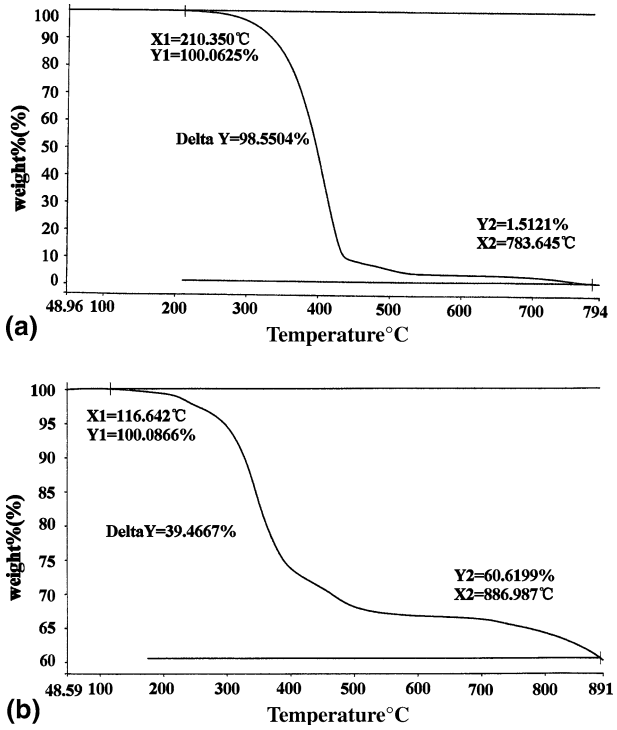

Fig. 6 Thermogravimetric analysis of (**a**) fresh and (**b**) used grease sample

According to above analysis, the greases used in bearing suffered heavily thermo-oxidation degradation due to high temperature during the bearing operation. A large amount of low-molecular compounds including carbonyl-containing degradation products were formed on the bearing raceway. The contents of grease were changed, and lubricating capacity of the grease were deteriorated. Consequently, the lubricant film in the roller/raceway contact could not be formed effectively, which would result in contact fatigue wear of the counterfaces and the formation of contact debris. Thus, by forcing the bearing to run under poor lubricating conditions, serious friction and wear were resulted.

Chemical Composition and Microscopic Features Analysis of the Inner-Ring Surface

In order to identify the features of the fracture process of the surfaces of the bearing the inner ring were examined.

Chemical Composition and Hardness Analysis

The chemical composition of the bearing materials was determined by photoelectric direct reading spectrometry. The results were shown in Table 1. It can be seen that the composition of the materials corresponded to the specified composition range. On the pieces cut out from the inner ring, the hardness (HRC) at different orientations was determined. The results showed that the distribution of the hardness values of the failed bearing inner-ring material ranged from 61 to 62 (HRC) and met the 60–64 HRC range requirement. These results demonstrate that the chemical composition and the average hardness of the bearing materials were qualified and consistent with the specifications for GCr15 bearing steel.

Microstructure Observation and Analysis

The wear indentations on the raceway of the bearing inner ring were detected using SEM and EDS. Figure 7a shows the surface of the wear zones was covered with a multitude of irregular pits. In order to further analyze the cause of pits, a magnified image of a single pit was observed and the composition within the pit was investigated as shown in Fig. 7b and c. It can be seen from Fig. 7b that the pit was formed by the removal of metal from the surface with no obvious surface plastic deformation. The pit had sides perpendicular to the contact surface and exhibited irregular shape. A number of cracks can be observed at and near the contact surface, which can be classified as the failure mode of surface rolling contact fatigue. The main chemical composition within the pit shows the presence of iron and

Table 1 Chemical composition of the bearing inner-ring material (wt.%)

	C	Si	Mn	P	S	Cr
	0.963	0.582	1.064	0.017	0.008	1.464
Specified	0.95–1.05	0.40–0.65	0.95–1.20	≤0.027	≤0.02	1.30–1.65

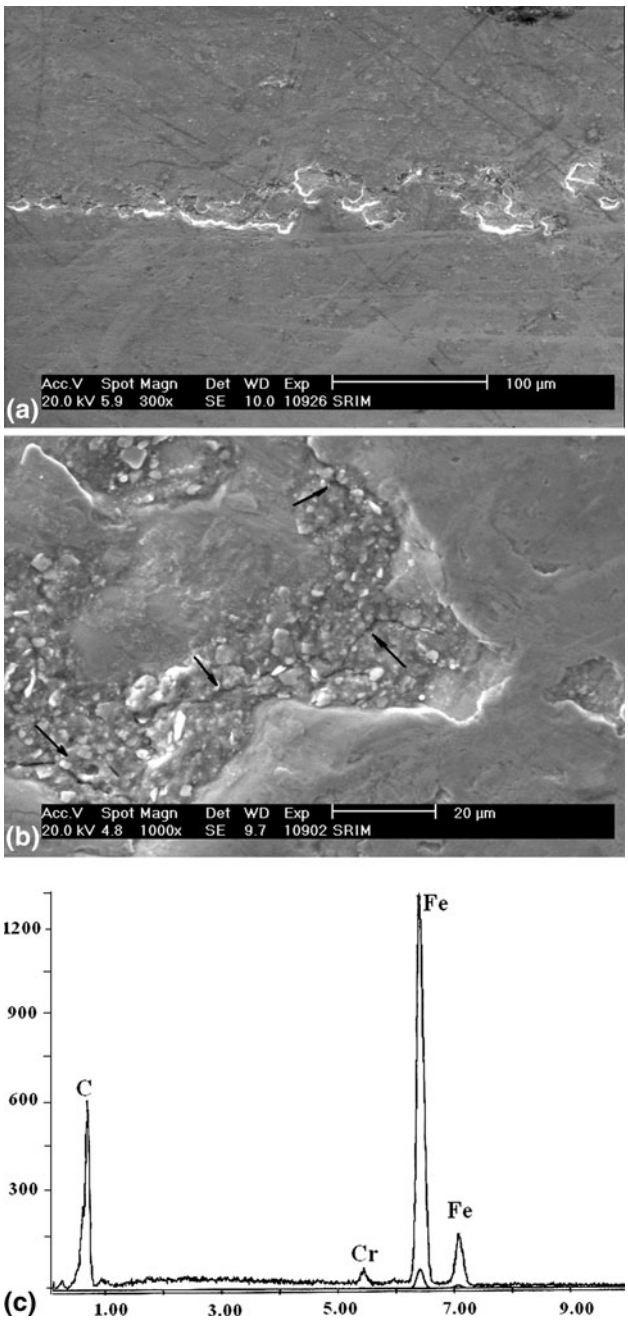

Fig. 7 SEM and EDS of wear pits of outer perimeter of bearing inner ring. (**a**) Irregular pits, (**b**) magnified image of a single pit, and (**c**) EDS of pit

chromium (see Fig. 7c), which was consistent with that of the bearing materials itself. It is further illustrated that formation of the pits had nothing to do with any kinds of corrosion, and was just resulted from wear due to poor lubrication.

Eichler et al. [15] stated that a bearing running under a well-lubricated condition benefits from a lubricant film which could completely separates the two counterfaces. Namely, there was no contact operating under elasto-hydrodynamic lubrication between the asperities and the bearing. However, if there is, or is likely to be contact between asperities, then the bearing is said to be running in the boundary lubrication regime. From the analysis in the "Characterizations of the Lubricating Grease" section, it is inferred that the chemical compositions of used grease were changed due to thermo-oxidation degradation, which led to a loss of lubricating capacity during the bearing operation. Consequently, the lubricant film in the roller/raceway contact was not formed effectively, and thus could not contribute to an effective separation of the contacting surfaces. Whenever two curved surfaces were in contact under load, the contact began to occur along a very small circular or elliptical area and resulted in the rolling contact fatigue with continued bearing operation.

Due to the damage of used grease structure, MoS_2 particles were aggregated in "sludge" on the damaged raceway surface or in the pits. Figure 8a shows the SEM micrograph of partial pits contained black particles, and Fig. 8b shows its EDS result. It can be seen that the composition of particle in the pits was mainly molybdenum and sulfur, while the presence of iron and chromium was mainly resulted from metallic wear debris from the matrix material of the bearing.

The formation of contact fatigue pits were accompanied by the occurrence of the wear debris. The bearing steel debris oxidized and formed the distinct red powder [16], which can in return cause abrasive wear. Figure 9a shows the SEM micrograph of the red-brown discolored zone on the outer perimeter of the inner ring of the bearing, and Fig. 9b shows the EDS results of the particles on the surface. As shown in Fig. 9a, there were large amounts of particulates on the discolored surface of the raceway with the parallel bands pattern. EDS analysis shows that the chemical composition of particulates was mainly iron and oxygen (see Fig. 9b, namely, iron oxides Fe_2O_3 (red-brown particulates). The bands show the position where the bearing surface was subjected to sliding and thus wear. These particulates further acted as stress concentration sites and accelerated the initiation of surface cracks. Under rolling and rolling-sliding contact fatigue, flaking occurred

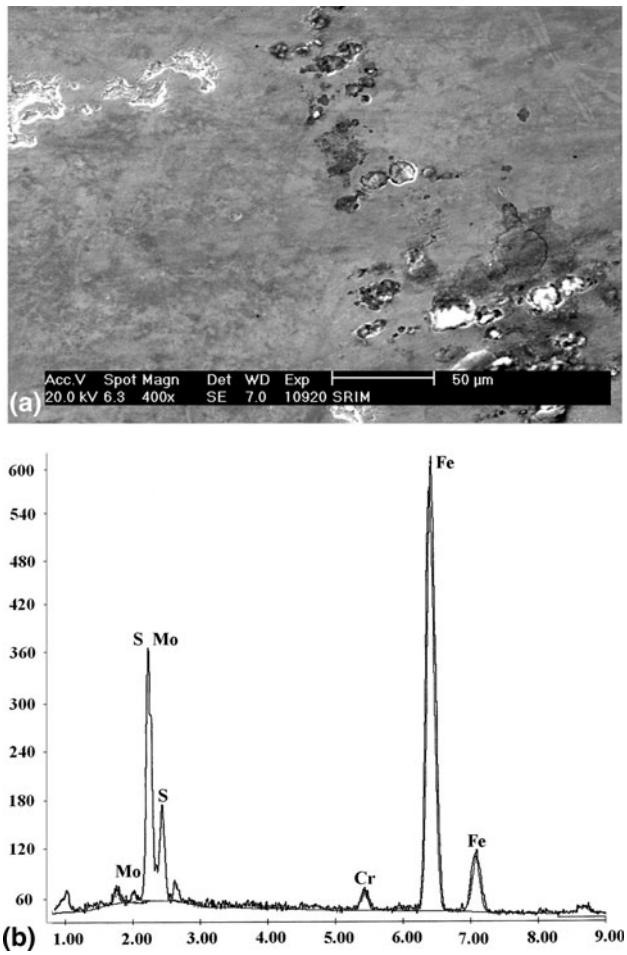

Fig. 8 SEM and EDS of partial pits contained black particles. (**a**) Pits contained black particles and (**b**) EDS of black particles

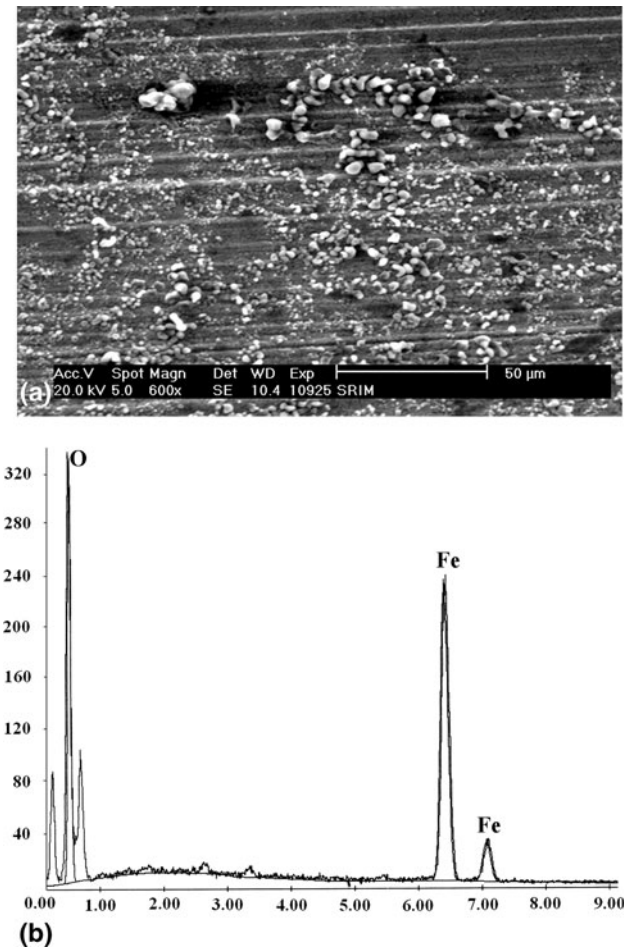

Fig. 9 SEM and EDS of red-brown discolored zone on the outer perimeter of bearing inner ring (**a**) particulates and bands (**b**) EDS of particulates

as a progression of the pits [3], and led to the formation of large, irregular-shaped pits which caused rapid failure of the bearing.

Conclusions and Remedial Measures

1. The generation of cracks at or near the contact surface and presence of flaky wear particles and irregular-shaped pits provided conclusive evidences for surface contact fatigue. This evidence was found through detailed electron microscopic investigations of the damaged surface of the inner ring of the bearing. The dominant mode of the bearing failure was surface contact fatigue between the rollers and the raceways.
2. During operation of the bearing, the lubricating greases suffered heavily thermo-oxidation degradation due to high temperature. The chemical compositions of greases were changed, which led to a loss of lubricating capacity and failure of the greases. The lubricating film in the roller/raceway contact cannot be effectively formed, which resulted in direct contact friction between the two counterfaces and occurrence of surface contact fatigue damage.
3. Due to damage of the grease structure, MoS_2 particulates under rolling and rolling-sliding contact were aggregated by "sludge" on the raceways. The wear debris and pits acted as stress concentration sites. These geometric inhomogeneities led to highly localized stresses, rapid crack initiation, and the formation of contact fatigue pits. Under continued operation, the pitting/fatigue progress caused flaking. This resulted in the formation of large, irregular pits and the accumulation of debris which cause rapid deterioration and failure of the bearing.
4. To extend the lifetime of the bearing, probably the best countermeasure is to replace the lubricating greases and choose temperature resistant, antioxidant lubricating grease such as RD-1, which is a high-temperature composite grease. In addition, shortening the cycle of lubricant replenishment in the track of the bearing is

probably the simplest approach for ensuring a bearing running under a well-lubricated condition all the time.

Acknowledgments This investigation was supported by Shanghai Leading Academic Discipline Project, Project Number B113. The support is gratefully acknowledged.

References

1. Zhou, Z.X.: 滚动轴承常见失效形式分析与正确维护 (Common failure type analysis of rolling bearing and its correct maintenance). Constr. Mach. 9, 67–71 (2003) (in Chinese)
2. Li, Y.J., Tao, C.H., Zhang, W.F., et al.: Fracture analysis on cage rivets of a cylindrical roller bearing. Eng. Fail. Anal. **15**(6), 796–801 (2008) (in English)
3. Fernandes, P.J.L.: Contact fatigue in rolling-element bearings. Eng. Fail. Anal. (4), 155–160 (1997) (in English)
4. Yang, W.Q., Chen, Y.Z.: 减少电动机滚动轴承故障的途径 (Methods for reducing the faults in rolling contact bearing of motor). Explos. Proof Electr. Mach. **40**(2), 28–30 (2005) (in Chinese)
5. Carré, D.J., Bauer, R., Fleischauer, P.D.: Chemical analysis of hydrocarbon grease from spin-bearing tests. ASLE Trans. **26**, 475–480 (1983) (in English)
6. Tomaru, M., Suzuki, T., Ito, H., Suzuki, T.: Grease-life estimation and grease deterioration in sealed ball bearings. In: Proc. JSLE Int. Trib. Conf., 1985, pp. 1039–1044 (in English)
7. Hosoya, S., Hayano, M.: Deterioration of lithium soap greases and functional life in ball bearings. NLGI Spokesm. **53**, 246–251 (1989) (in English)
8. Cann, P.M., Doner, J.P., Webster, M.N., Wickstrom, V.: Grease degradation in rolling element bearings. STLE Trans. **44**, 399–404 (2001) (in English)
9. Cann, P.M.: Grease degradation in a bearing simulation device. Trib. Int. **39**, 1698–1706 (2006) (in English)
10. Komatsuzaki, S., Uematsu, T., Kobayashi, Y.: Change of grease characteristics to the end of lubricating life. NLGI Spokesm. **63**, 22–27 (2000) (in English)
11. Fernandes, P.J.L., Mcduling, C.: Surface contact fatigue failures in gears. Eng. Fail. Anal. **4**(2), 99–107 (1997) (in English)
12. ASM Metals Handbook, Failure of Rolling-Element Bearings, Vol. 11, Failure Analysis and Prevention, 9th edn. American Society for Metals, Metals Park, OH, pp. 490–513 (1986) (in English)
13. Xie, F., Yu, Y.P., Yao, J.B.: 脂的氧化与抑制 (Oxidation of grease and its inhibition). Synth. Lubr. **30**(3), 49–52 (2003) (in Chinese)
14. Xue, J., Zhang, J.Y., Wang, C.T.: 红外波谱技术在轴承润滑脂分析上的应用 (Application of infrared spectrum technique in bearing grease analysis). Bearing 7, 25–29 (2003) (in Chinese)
15. Eichler, J.W., Matthews, A., Leyland, A., et al.: The influence of coatings on the oil-out performance of rolling bearings. Surf. Coat. Technol. **202**, 1073–1077 (2007) (in English)
16. Berthier, Y., Vincent, L., Godet, M.: Fretting fatigue and fretting wear. Trib. Int. **22**, 235–242 (1989) (in English)